

# Analysis on the Langmuir Adsorption Isotherm of the Over-Potentially Deposited Hydrogen (OPD H) at the Polycrystalline Au | Acidic Aqueous Electrolyte Interface Using the Phase-Shift Method

Jang H. Chun\* and Sang K. Jeon

Mission Technology Research Center, Department of Electronic Engineering,  
Kwangwoon University, Seoul 139-701, Korea

(Received August 6, 2001 : Accepted August 20, 2001)

**Abstract.** The Langmuir adsorption isotherm of the over-potentially deposited hydrogen (OPD H) for the cathodic H<sub>2</sub> evolution reaction (HER) at the poly-Au|0.5 M H<sub>2</sub>SO<sub>4</sub> aqueous electrolyte interface has been studied using cyclic voltammetric and ac impedance techniques. The behavior of the phase shift ( $0^\circ \leq -\phi \leq 90^\circ$ ) for the optimum intermediate frequency corresponds well to that of the fractional surface coverage ( $1 \geq \theta \geq 0$ ) at the interface. The phase-shift profile ( $-\phi$  vs.  $E$ ) for the optimum intermediate frequency, i.e., the phase-shift method, can be used as a new method to estimate the Langmuir adsorption isotherm ( $\theta$  vs.  $E$ ) of the OPD H for the cathodic HER at the interface. At the poly-Au|0.5 M H<sub>2</sub>SO<sub>4</sub> electrolyte interface, the equilibrium constant ( $K$ ) and standard free energy ( $\Delta G_{ads}$ ) of the OPD H are  $2.3 \times 10^{-6}$  and  $32.2 \text{ kJ mol}^{-1}$ , respectively.

**초 록 :** 순환전압전류 및 교류임피던스 기법을 이용하여 다결정 0.5 M H<sub>2</sub>SO<sub>4</sub> 수용액 계면에서 음극 H<sub>2</sub>발생 반응을 위한 과전위 전착(흡착)된 수소의 Langmuir 흡착등온식을 연구조사 하였다. 다결정 Au|0.5 M H<sub>2</sub>SO<sub>4</sub> 수용액 계면에서, 최적중간주파수일 때 위상이동( $0^\circ \leq -\phi \leq 90^\circ$ ) 거동은 표면피복율( $1 \geq \theta \geq 0$ ) 거동에 정확하게 상응한다. 최적중간주파수일 때 위상이동 변화( $-\phi$  vs.  $E$ ) 즉 위상이동 방법은 다결정 Au|0.5 M H<sub>2</sub>SO<sub>4</sub> 수용액 계면에서 음극 H<sub>2</sub>발생 반응을 위한 과전위 전착(흡착)된 수소의 Langmuir 흡착등온식( $\theta$  vs.  $E$ )을 추정할 수 있는 새로운 방법으로 사용될 수 있다. 다결정 Au|0.5 M H<sub>2</sub>SO<sub>4</sub> 수용액 계면에서, 과전위 전착(흡착)된 수소의 흡착평형상수( $K$ )와 표준자유에너지( $\Delta G_{ads}$ )는 각각  $2.3 \times 10^{-6}$ 과  $32.2 \text{ kJ mol}^{-1}$ 이다.

**Key words :** Phase-shift method; Langmuir adsorption isotherm; Over-potentially deposited hydrogen; Gold electrodes

## 1. Introduction

The kinetics and mechanisms of the cathodic H<sub>2</sub> evolution reaction (HER) at noble metal (Pt, Ir, Rh, Au, Pd) | aqueous electrolyte interfaces have been extensively and intensively studied in interfacial electrochemistry. Many electrochemical methods and analyses on the H adsorption sites and processes for the cathodic HER at the noble metal | aqueous electrolyte interfaces are described and reviewed elsewhere.<sup>1-8)</sup> Especially, the cyclic voltammetric and electrochemical impedance spectroscopic methods have been extensively used to study the cathodic HER at the interfaces. However, it seems to be that the phase-shift profile for the optimum intermediate frequency, i.e., the phase-shift method, has not been used to study the H adsorption sites and processes at the interfaces.

The relation, transition, and criterion of the under-potentially deposited hydrogen (UPD H) and the over-potentially deposited hydrogen (OPD H) are necessary and important to understand the kinetics and mechanisms of the cathodic HER.<sup>2,4,6-17)</sup> It is well known that the UPD H and the OPD H

occupy different surface adsorption sites and act as two distinguishable electroadsorbed H species. And only the OPD H can contribute to the cathodic HER. However, the relation, transition, and criterion of the UPD H and the OPD H at the noble metal | aqueous electrolyte interfaces have been studied on a point of view of the H<sub>2</sub> evolutions and potentials rather than the H adsorption sites and processes, i.e., the Langmuir adsorption isotherms.

The Langmuir adsorption isotherm is based on the kinetics and thermodynamics of the electrode interfaces. Although the Langmuir adsorption isotherm may be regarded a classical model and theory in physical electrochemistry,<sup>18)</sup> it is useful and effective to study the H adsorption sites and processes for the cathodic HER at the interfaces. Thus, there is a need in the art for a fast, simple, and reliable technique to estimate or determine the Langmuir adsorption isotherms for characterizing the OPD H for the cathodic HER at the Au | acidic aqueous electrolyte interfaces.

Recently, we have experimentally and consistently found that the phase-shift method can be effectively used to estimate the Langmuir or the Frumkin adsorption isotherms of the UPD H and the OPD H for the cathodic HER at the interfaces.<sup>19-22)</sup> Although the proposition of the phase-shift

\*E-mail: jhchun@daisy.kwangwoon.ac.kr

method is not based on the kinetics or the thermodynamics, it is useful and effective for studying the relation, transition, and criterion between the UPD H and the OPD H for the cathodic HER at the noble metal | aqueous electrolyte interfaces.

In this paper we will represent the Langmuir adsorption isotherm of the OPD H for the cathodic HER at the poly-Au | 0.5 M  $\text{H}_2\text{SO}_4$  aqueous electrolyte interface using the phase-shift method. It appears that the phase-shift method is useful and effective to estimate or determine the Langmuir adsorption isotherm and to study the electrode kinetics at the interface.

## 2. Experimental

### 2.1. Preparations

Taking into account  $\text{H}^+$  concentrations and effects of pH,<sup>23)</sup> an acidic aqueous electrolyte was prepared from  $\text{H}_2\text{SO}_4$  (Junsei, special grade) with purified water (resistivity:  $> 18 \text{ M}\Omega \text{ cm}$ ) obtained from a Millipore system. The 0.5 M  $\text{H}_2\text{SO}_4$  aqueous electrolyte was deaerated with 99.999% purified nitrogen gas for 10 min before the experiments.

A standard 3-electrode configuration was employed using an SCE reference electrode and a poly-Au wire (Johnson Matthey, purity: 99.999%, 1 mm diameter, surface area:  $\sim 0.57 \text{ cm}^2$ ) working electrode. The poly-Au working electrode was prepared by flame cleaning and then quenched in the Millipore Milli-Q water. A Pt wire (Johnson Matthey, purity: 99.95%, 1.5 mm diameter) was used as a counter electrode. The working and counter electrodes were separately placed ( $\sim 4 \text{ cm}$ ) in the same compartment Pyrex cell using Teflon holders.

### 2.2. Measurements

Cyclic voltammetric (scan potential:  $-0.30$  to  $1.65 \text{ V vs. SCE}$ , scan rate:  $200 \text{ mV s}^{-1}$ ) and ac impedance (single sine wave, scan frequency:  $10^4$  to  $1 \text{ Hz}$ , ac amplitude:  $5 \text{ mV}$ , dc potential:  $0$  to  $-0.575 \text{ V vs. SCE}$ ) techniques were used to study the relation between the phase-shift profile for the optimum intermediate frequency and the corresponding Langmuir adsorption isotherm.

The cyclic voltammetric experiment was performed using an EG&G PAR Model 273A potentiostat controlled with the PAR Model 270 software package. The ac impedance experiment was performed using the same apparatus in conjunction with a Schlumberger SI 1255 HF Frequency Response Analyzer controlled with the PAR Model 388 software package. In order to obtain comparable and reproducible results, all measurements were carried out using the same preparations, procedures, and conditions at room temperature. The international sign convention is used, i.e., cathodic currents and lagged phase shifts or angles are taken as negative.

## 3. Results and Discussion

### 3.1. The cyclic voltammogram

Fig. 1 shows the typical cyclic voltammogram of the

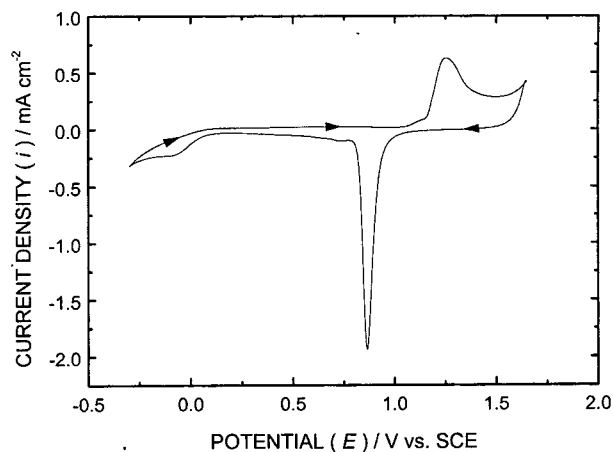


Fig. 1. The typical cyclic voltammogram at the poly-Au | 0.5 M  $\text{H}_2\text{SO}_4$  electrolyte interface. Surface area:  $\sim 0.57 \text{ cm}^2$ . Scan potential:  $-0.30$  to  $1.65 \text{ V vs. SCE}$ . Scan rate:  $200 \text{ mV s}^{-1}$ . 10th scan.

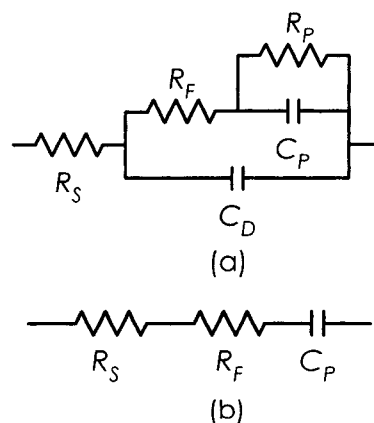


Fig. 2. (a) The equivalent circuit for the cathodic  $\text{H}_2$  evolution reaction at the poly-Au | 0.5 M  $\text{H}_2\text{SO}_4$  electrolyte interface and (b) The simplified equivalent circuit for the intermediate frequencies at the interface.

steady state at the poly-Au | 0.5 M  $\text{H}_2\text{SO}_4$  aqueous electrolyte interface. As pointed out by Jerkiewicz *et al.*,<sup>24-25)</sup> the UPD H peak is not experimentally observable at the interface. However, the plateau due to the UPD H occurs at ca.  $-0.10$  to  $-0.162 \text{ V vs. SCE}$ . It implies that the Langmuir adsorption isotherm of the UPD H is not experimentally observable at the cathode potential range.<sup>22,23)</sup> The anionic adsorption effects on the plateau have not been considered.<sup>7,17)</sup> Generally, the UPD H peak and the corresponding cathode potential are necessary and useful to verify the Langmuir adsorption isotherm of the UPD H or the OPD H for the cathodic HER at the interface.

### 3.2. Phase-shift profile for the optimum intermediate frequency

Various equivalent circuits were proposed to model the frequency responses of the interfaces for intermediate adsorptions under different conditions.<sup>10,14,26-31)</sup> The equivalent circuit for the cathodic HER is usually expressed as shown in Fig. 2(a).<sup>10,14,26,29,31)</sup> Taking into account the relaxation time effect

on the ac impedance experiment,<sup>10,32)</sup> the equivalent circuit elements shown in Fig. 2(a) are defined as:  $R_S$  is the electrolyte resistance,  $R_F$  is the equivalent circuit element of the faradaic resistance ( $R_\phi$ ) for the discharge reaction,  $R_p$  is the equivalent circuit element of the faradaic resistance for the recombination reaction,  $C_p$  is the equivalent circuit element of the adsorption pseudocapacitance ( $C_\phi$ ), and  $C_D$  is the double-layer capacitance.

The two equivalent circuit elements, i.e.,  $R_F$  and  $C_p$  are the equivalent resistance and capacitance associated with the adsorption processes of the UPD H and/or the OPD H, respectively. Under the ac impedance experiment,  $R_F$  is similar to  $R_\phi$  but is not equal to  $R_\phi$ . In general,  $R_F$  is smaller than  $R_\phi$  due to the relaxation times of the previously adsorbed H, i.e., the UPD H and/or the OPD H, on the electrode surface. Also,  $C_p$  is similar to  $C_\phi$  but is not equal to  $C_\phi$ . In general,  $C_p$  is greater than  $C_\phi$  due to the relaxation times of the previously adsorbed H, i.e., the UPD H and/or the OPD H, on the electrode surface. It implies that the behavior of  $R_F$  and  $C_p$  depends strongly on that of  $R_\phi$  and  $C_\phi$ . Therefore, the adsorption processes of the UPD H and/or the OPD H corresponding to the combination of  $R_F$  and  $C_p$  can be correctly expressed in terms of the phase delay. This aspect was not well interpreted in the previously published papers.<sup>19-21)</sup> Of course, the experimental results presented there and related discussions are unchanged. This is discussed in more detail later.

At low frequencies, the equivalent circuit can be expressed as a serial connection of  $R_S$ ,  $R_F$ , and  $R_p$ . At high frequencies, the equivalent circuit can be expressed as a serial connection of  $R_S$  and  $C_D$ . At intermediate frequencies, the equivalent circuit can be simplified as a serial connection of  $R_S$ ,  $R_F$ , and  $C_p$  shown in Fig. 2(b). Since, practically,  $C_p$  is greater than  $C_D$ . However, it implies that the simplified equivalent circuit for the intermediate frequencies can be applied to the poly-Au|0.5 M H<sub>2</sub>SO<sub>4</sub> electrolyte interface regardless of H<sub>2</sub> evolution. In other words, it is valid and effective for studying the UPD H and/or the OPD H at the interface. The frequency responses of the equivalent circuit shown in Fig. 2(a) are described elsewhere.<sup>26-30)</sup>

From the simplified equivalent circuit for the intermediate frequencies shown in Fig. 2(b), the corresponding phase shift or angle ( $\phi$ ) can be derived as follows:

$$\phi = -\tan^{-1}[1/\omega(R_S + R_F)C_p] \quad (1)$$

$$R_F \propto R_\phi (< R_\phi) \text{ and } C_p \propto C_\phi (> C_\phi) \quad (2)$$

$$C_\phi = \gamma(d\theta/dE) \quad (3)$$

where  $\omega (= 2\pi f)$  is the angular frequency,  $R_\phi$  is the faradaic resistance for the discharge reaction of the UPD H or the OPD H,  $C_\phi$  is the adsorption pseudocapacitance for the Langmuir adsorption conditions,  $\gamma$  is the charge corresponding to the saturation coverage of  $\theta$ ,  $\theta$  is the fractional surface coverage of the UPD H or the OPD H, and  $E$  is the applied dc potential. A minus sign shown in Eq. (1) implies a lagged

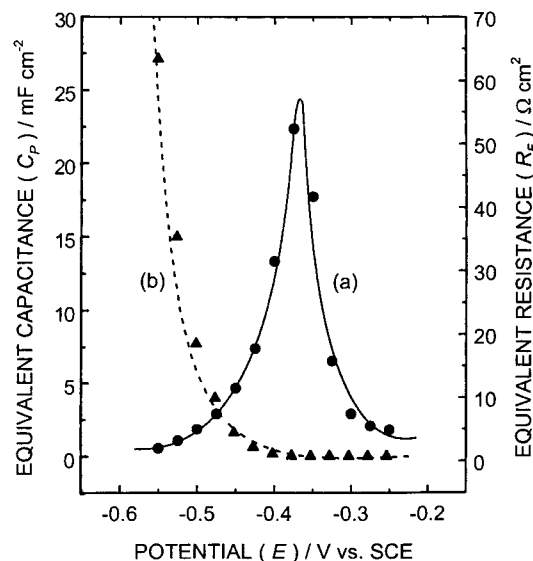


Fig. 3. The profiles of the measured equivalent circuit elements ( $R_F$ ,  $C_p$ ) respect to  $E$  for the optimum intermediate frequency (ca. 100 Hz) at the poly-Au|0.5 M H<sub>2</sub>SO<sub>4</sub> electrolyte interface. Single sine wave. Scan frequency: 10<sup>4</sup> to 1 Hz. ac amplitude: 5 mV. dc potential: -0.25 to -0.55 V vs. SCE. (a) Equivalent resistance ( $R_F$ ) and (b) Equivalent capacitance ( $C_p$ ).

phase. From Eq. (1), it is readily understood that the lagged phase depends strongly on  $R_F$  and  $C_p$ , i.e.,  $R_\phi$  and  $C_\phi$  or  $\theta$ . In other words, the phase shift ( $-\phi$ ) depends markedly on the adsorption processes of the UPD H and/or the OPD H at the interface. However, as previously described, it should not be confused  $C_p$  with  $C_\phi$  which has a maximum value at  $\theta = 0.5$  and can be neglected at  $\theta \approx 0$  and 1.<sup>10,26,29,31)</sup>

Figs. 3(a) and (b) show the profiles of the measured  $R_F$  and  $C_p$  respect to  $E$  for the optimum intermediate frequency (ca. 100 Hz) at the poly-Au|0.5 M H<sub>2</sub>SO<sub>4</sub> electrolyte interface, respectively. As previously described, Fig. 3(a) shows that  $R_F$  is smaller than  $R_\phi$ . Since, the left-hand side of the profile is lower than the right-hand side of the profile. It is attributed to the increase of H<sup>+</sup>, i.e., the relaxation time effect, at the interface. On the other hand, as previously described, Fig. 3(b) shows that  $C_p$  is greater than  $C_\phi$ . Since, the profile of  $C_p$  increases from the right-hand side to the left-hand side, i.e., towards more negative potentials. Similarly, it is attributed to the increase of H<sup>+</sup>, i.e., the relaxation time effect, at the interface. However, it should be noted that the equivalent resistance profile ( $R_F$  vs.  $E$ ) shown in Fig. 3(a) has the peak due to the Langmuir adsorption process. On the other hand, the equivalent capacitance profile ( $C_p$  vs.  $E$ ) shown in Fig. 3(b) has not the peak. It implies that the H<sup>+</sup> at the interface increases consistently with increase of the applied dc potential, i.e., the cathode potential ( $E$ ). As previously described, it is attributed to the superposition of the Langmuir adsorption process and the relaxation time effect at the interface. Fig. 3(b) also shows that  $C_p$  increases rapidly beyond the peak potential (ca. -0.37 V vs. SCE) of the equivalent resistance profile ( $R_F$  vs.  $E$ ). It is understood that  $C_\phi$  has a maximum value at the peak potential due to the Langmuir

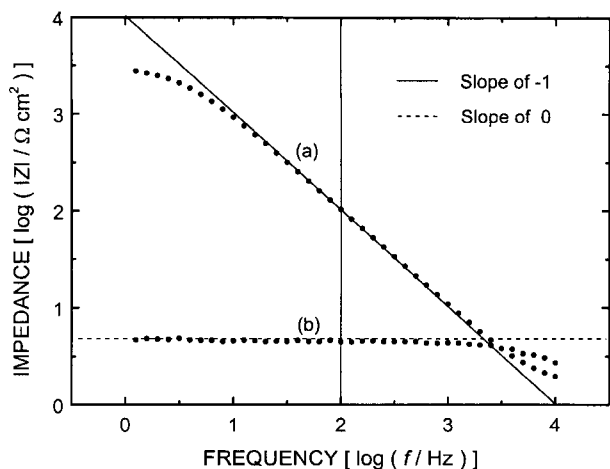


Fig. 4. The comparison of the two extremely distinguishable frequency response curves at the poly-Au | 0.5 M H<sub>2</sub>SO<sub>4</sub> electrolyte interface. Vertical solid line: ca. 100 Hz. Single sine wave. Scan frequency: 10<sup>4</sup> to 1 Hz. ac amplitude: 5 mV. dc potential: (a) -0.30 V and (b) -0.55 V vs. SCE.

adsorption process. The determination of the optimum intermediate frequency is discussed in more detail later. Consequently, it can be interpreted that the relaxation time effect on  $R_F$  and  $C_P$  is not conflicting to analyze the H adsorption processes at the interface.

From Figs. 2(b), 3, and Eq. (1), it is understood that the adsorption processes of the UPD H and/or the OPD H at the interface can be expressed in terms of the lagged phase. Practically,  $R_F$  is much greater than  $R_S$  and so the phase shift ( $-\phi$ ) can be substantially determined by the serial connection of  $R_F$  and  $C_P$  i.e.,  $R_\phi$  and  $C_\phi$  or  $\theta$ . It implies that the behavior of the phase shift ( $0^\circ \leq -\phi \leq 90^\circ$ ) for the optimum intermediate frequency can be related to that of the fractional surface coverage ( $1 \geq \theta \geq 0$ ). In other words, the change rate of  $\Delta(-\phi)/\Delta E$  or  $d(-\phi)/dE$  corresponds well to that of  $\Delta\theta/\Delta E$  or  $d\theta/dE$ . This is discussed in more detail later. However, it appears that the mathematical relation between the phase shift ( $-\phi$ ) and the fractional surface coverage ( $\theta$ ) has not been derived or reported elsewhere.

Fig. 4 shows the comparison of the two extremely distinguishable frequency responses at the poly-Au | 0.5 M H<sub>2</sub>SO<sub>4</sub> electrolyte interface. The absolute value of the impedance vs. the frequency ( $|Z|$  vs.  $f$ ) is plotted on a log-log scale. In Fig. 4(a), the slope portion of the frequency response curve represents the capacitive behavior of the poly-Au | 0.5 M H<sub>2</sub>SO<sub>4</sub> electrolyte interface. Since, a slope of -1 represents the ideal capacitive behavior. It implies that  $C_P$  has a minimum value as shown in Fig. 3(b). It also implies that  $\theta$  can be set zero as shown in Table 1. Therefore, from Eq. (1),  $-\phi$  has a maximum value ( $\leq 90^\circ$ ) as shown in Fig. 5(a) and Table 1. On the other hand, in Fig. 4(b), the horizontal portion of the frequency response curve represents the resistive behavior of the poly-Au | 0.5 M H<sub>2</sub>SO<sub>4</sub> electrolyte interface. Since, a slope of zero represents the ideal resistive behavior. It implies that the H adsorption at the interface is almost saturated. In other words,  $C_P$  has a maximum value as shown in Fig. 3(b). It

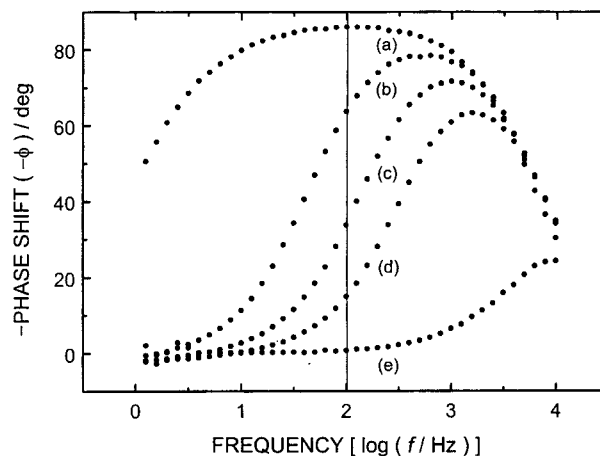


Fig. 5. The comparison of the phase-shift curves at the poly-Au | 0.5 M H<sub>2</sub>SO<sub>4</sub> electrolyte interface. Vertical solid line: ca. 100 Hz. Single sine wave. Scan frequency: 10<sup>4</sup> to 1 Hz. ac amplitude: 5 mV. dc potential: (a) -0.25 V, (b) -0.35 V, (c) -0.375 V, (d) -0.40 V, and (e) -0.55 V vs. SCE.

Table 1. The measured phase shift ( $-\phi$ ) for the optimum intermediate frequency (ca. 100 Hz) and the estimated fractional coverage ( $\theta$ ) at the poly-Au | 0.5 M H<sub>2</sub>SO<sub>4</sub> electrolyte interface

E (V vs. SCE)	$-\phi$ (deg)	$\theta^a$
-0.250	86.1	$\approx 0$
-0.275	86.0	0.001
-0.300	85.0	0.013
-0.325	80.4	0.067
-0.350	63.7	0.263
-0.375	33.8	0.630
-0.400	15.0	0.833
-0.425	7.4	0.923
-0.450	4.2	0.960
-0.475	2.4	0.981
-0.500	1.6	0.991
-0.525	1.1	0.996
-0.550	0.8	$\approx 1$

<sup>a</sup>Estimated using the measured phase shift ( $-\phi$ ).

implies that  $\theta$  can be set unity as shown in Table 1. Therefore, from Eq. (1),  $-\phi$  has a minimum value ( $\geq 0^\circ$ ) as shown in Fig. 5(e) and Table 1.

Fig. 5 shows the comparison of the phase-shift curves ( $-\phi$  vs.  $f$ ) for the different cathode potentials at the poly-Au | 0.5 M H<sub>2</sub>SO<sub>4</sub> electrolyte interface. In Fig. 5, it should be noted that the phase-shift curves and phase angles are markedly characterized at the intermediate frequencies. The center frequency (ca. 100 Hz) of a slope of 1 shown in Fig. 4(a), i.e., the center frequency of the intermediate frequencies (ca. 30 to 300 Hz), can be set as the optimum intermediate frequency for the phase-shift profile ( $-\phi$  vs.  $E$ ). Of course, the exactly same phase-shift profile can also be obtained at ca. 30 and 300 Hz, i.e., the range of the intermediate frequencies. The determination of the optimum intermediate frequency for the

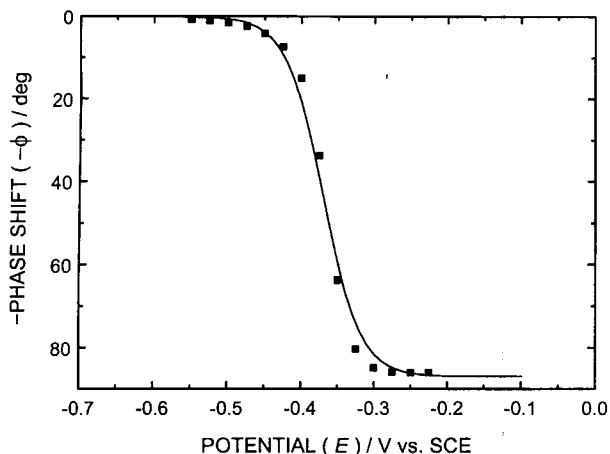


Fig. 6. The phase-shift profile ( $-\phi$  vs.  $E$ ) for the optimum intermediate frequency (ca. 100 Hz) at the poly-Au | 0.5 M  $\text{H}_2\text{SO}_4$  electrolyte interface.

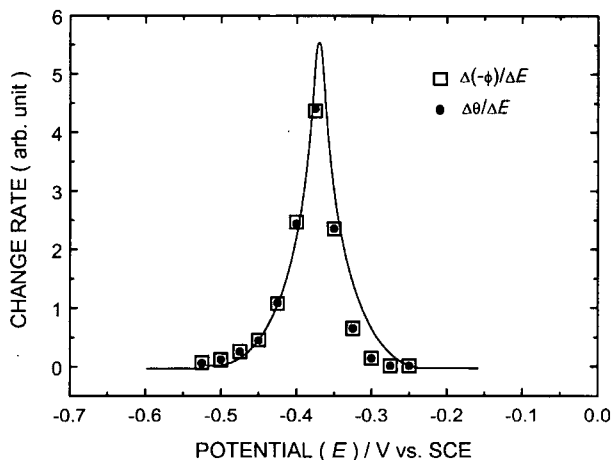


Fig. 7. The comparison of the change rates of the  $\Delta(-\phi)/\Delta E$  and the  $\Delta\theta/\Delta E$  for the optimum intermediate frequency (ca. 100 Hz) at the poly-Au | 0.5 M  $\text{H}_2\text{SO}_4$  electrolyte interface.

phase-shift profile is described elsewhere.<sup>19,20,33</sup> Finally, the cathode potentials and the corresponding phase shifts for the optimum intermediate frequency (ca. 100 Hz) can be plotted as the phase-shift profile ( $-\phi$  vs.  $E$ ) shown in Fig. 6.

Fig. 7 shows the comparison of the change rates of the  $-\phi$  vs.  $E$  and the  $\theta$  vs.  $E$ , i.e., the  $\Delta(-\phi)/\Delta E$  or  $d(-\phi)/dE$  and the  $\Delta\theta/\Delta E$  or  $d\theta/dE$ , at the poly-Au | 0.5 M  $\text{H}_2\text{SO}_4$  electrolyte interface. The derivation of the  $\Delta(-\phi)/\Delta E$  and the  $\Delta\theta/\Delta E$  is based on the experimental data shown in Table 1. As expected, Table 1 and Fig. 7 show that both the  $\Delta(-\phi)/\Delta E$  or  $d(-\phi)/dE$  and the  $\Delta\theta/\Delta E$  or  $d\theta/dE$  are maximized at  $\theta = 0.5$  and are minimized at  $\theta \approx 0$  and 1. Fig. 7 also shows that the  $\Delta(-\phi)/\Delta E$  or  $d(-\phi)/dE$  corresponds well to the  $\Delta\theta/\Delta E$  or  $d\theta/dE$ . In other words, the behavior of the phase shift ( $0^\circ \leq -\phi \leq 90^\circ$ ) corresponds well to that of the fractional surface coverage ( $1 \geq \theta \geq 0$ ). Also, it should be noted that Figs. 3(a) and 7 are similar to the typical shape of the adsorption pseudocapacitance ( $C_\phi$ ) for the Langmuir adsorption conditions.<sup>10,26,29,30</sup> As previously described, it implies that the relaxation time

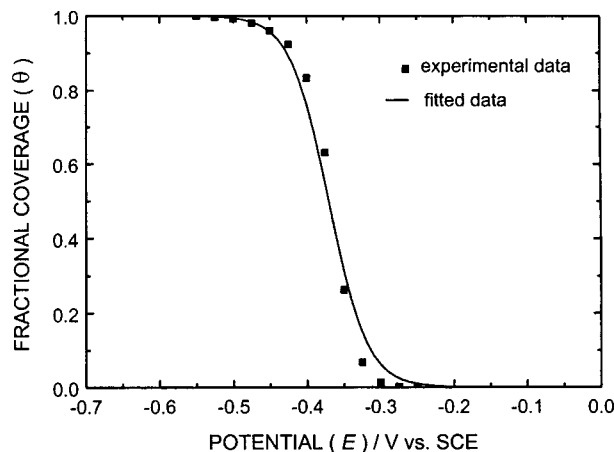


Fig. 8. The comparison of the experimental and fitted data for the Langmuir adsorption isotherm ( $\theta$  vs.  $E$ ) at the poly-Au | 0.5 M  $\text{H}_2\text{SO}_4$  electrolyte interface.  $K = 2.3 \times 10^{-6}$  (OPD H).

effect on  $R_F$  and  $C_P$  can be neglected to analyze or estimate the adsorption processes of the UPD H and/or the OPD H at the interface. In other words, the lagged phase described in Eq. (1) depends strongly on  $R_\phi$  and  $C_\phi$ , i.e.,  $\theta$ . For the Frumkin adsorption process, both the  $\Delta(-\phi)/\Delta E$  or  $d(-\phi)/dE$  and the  $\Delta\theta/\Delta E$  or  $d\theta/dE$  will be changed depending on the interaction parameter. Consequently, it can be interpreted that the phase-shift profile ( $-\phi$  vs.  $E$ ) for the optimum intermediate frequency corresponds well to the Langmuir adsorption isotherm ( $\theta$  vs.  $E$ ) at the interface regardless of  $\text{H}_2$  evolution.

### 3.3. Langmuir adsorption isotherm

The Langmuir adsorption isotherm is based on the assumptions that the surface is homogeneous and that lateral interaction effects are negligible. The hydrogen evolution reactions under the Langmuir adsorption conditions are described elsewhere.<sup>34</sup> Considering the application of the Langmuir adsorption isotherm to the formation of H on the poly-Au surface, the Langmuir adsorption isotherm can be expressed as follows:<sup>35</sup>

$$[\theta(1 - \theta)] = K C_{\text{H}^+} [\exp(-EF/RT)] \quad (4)$$

where  $\theta$  is the fractional surface coverage of the UPD H or the OPD H,  $K$  is the equilibrium constant for the UPD H or the OPD H,  $C_{\text{H}^+}$  is the  $\text{H}^+$  concentration in the bulk electrolyte,  $E$  is the applied dc potential, i.e., the cathode potential,  $F$  is the Faraday constant,  $R$  is the gas constant, and  $T$  is the absolute temperature.

At the poly-Au | 0.5 M  $\text{H}_2\text{SO}_4$  aqueous electrolyte (pH 0.62) interface, the fitted data, i.e., the calculated Langmuir adsorption isotherm using Eq. (4), are shown in Fig. 8. As expected, the Langmuir adsorption isotherm ( $\theta$  vs.  $E$ ) shown in Fig. 8 corresponds well to the phase-shift profile ( $-\phi$  vs.  $E$ ) for the optimum intermediate frequency shown in Fig. 6. From Fig. 8, it can be easily inferred that  $K = 2.3 \times 10^{-6}$  is applicable to the formation of H at the interface. Under the same conditions, Fig. 9 shows the numerically calculated

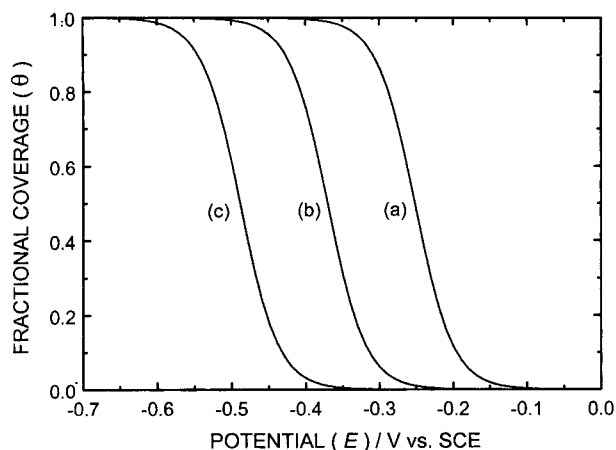


Fig. 9. The three numerically calculated Langmuir adsorption isotherms ( $\theta$  vs.  $E$ ) at the poly-Au | 0.5 M  $\text{H}_2\text{SO}_4$  electrolyte interface. (a)  $K = 2.3 \times 10^{-4}$ , (b)  $K = 2.3 \times 10^{-6}$ , and (c)  $K = 2.3 \times 10^{-8}$ .

Langmuir adsorption isotherms ( $\theta$  vs.  $E$ ) for three different values of  $K = 2.3 \times 10^{-4}$ ,  $2.3 \times 10^{-6}$ , and  $2.3 \times 10^{-8}$ .

The Langmuir adsorption isotherm shown in Fig. 8 is attributed to the OPD H. As previously described, the Langmuir adsorption isotherm due to the UPD H is not observed at the cathode potential range. It is understood that the adsorption sites of the UPD H are almost masked due to a high  $\text{H}^+$  concentration of the 0.5 M  $\text{H}_2\text{SO}_4$  electrolyte and/or the anionic adsorption effects under the steady state conditions.<sup>7-9,12,13,15,17,20-22</sup> Also, it should be noted that the experimental data shown in Figs. 3-8 and Table 1 are observed beyond the plateau and the corresponding cathode potential range (ca. -0.10 to -0.162 V vs. SCE) shown in Fig. 1. In other words, the Langmuir adsorption isotherm of the OPD H is located beyond the cathode potential range of the plateau. Of course, the Langmuir adsorption isotherm of the UPD H can be easily observed in alkaline aqueous electrolytes.<sup>20-22</sup>

Under the Langmuir adsorption conditions, the relation between the equilibrium constant ( $K$ ) for H adsorption (UPD H, OPD H) and the standard free energy ( $\Delta G_{ads}$ ) of H adsorption (UPD H, OPD H) is given using,<sup>35</sup> as

$$2.3RT \log K = -\Delta G_{ads} \quad (5)$$

At the poly-Au | 0.5 M  $\text{H}_2\text{SO}_4$  electrolyte interface, it is readily calculated using Eq. (5) that  $\Delta G_{ads}$  is 32.2 kJ mol<sup>-1</sup> for  $K = 2.3 \times 10^{-6}$  (OPD H).

## Conclusions

The phase-shift method for the Langmuir adsorption isotherm of the OPD H for the cathodic HER is proposed. The simplified equivalent circuit for the optimum intermediate frequency and the corresponding phase-shift equation are well fitted to the poly-Au | 0.5 M  $\text{H}_2\text{SO}_4$  aqueous electrolyte interface regardless of  $\text{H}_2$  evolution. The behavior of the phase shift ( $0^\circ \leq -\phi \leq 90^\circ$ ) for the optimum intermediate frequency corresponds well to that of the fractional surface coverage (1

$\geq \theta \geq 0$ ) at the interface. The phase-shift profile ( $-\phi$  vs.  $E$ ) for the optimum intermediate frequency, i.e., the phase-shift method, can be effectively used as a new method to estimate the Langmuir adsorption isotherm ( $\theta$  vs.  $E$ ) of the OPD H for the cathodic HER at the interface. At the poly-Au | 0.5 M  $\text{H}_2\text{SO}_4$  electrolyte interface, the equilibrium constant ( $K$ ) and standard free energy ( $\Delta G_{ads}$ ) of the OPD H are  $2.3 \times 10^{-6}$  and 32.2 kJ mol<sup>-1</sup>, respectively.

## Acknowledgements

The authors thank Dr. Mu. S. Cho (The First President of Kwangwoon University, Seoul, Korea) for supporting the EG & G PAR 273A Potentiostat/Galvanostat, Schlumberger SI 1255 HF FRA, and software packages. The authors would also like to thank Professor G. Jerkiewicz (Universite de Sherbrooke, Quebec, Canada) for his valuable suggestions and encouragement.

## References

1. S. Trasatti, "Advances in Electrochemical Science and Engineering", H. Gerischer, C. T. Tobias, Editors, Vol. 2, 1, VCH, New York (1993).
2. J. Lipkowsky, P.N. Ross, Editors, "Structure of Electrified Interfaces", VCH, New York (1993).
3. E. Gileadi, *Electrode Kinetics*, 164, VCH, New York (1993).
4. B. E. Conway, G. Jerkiewicz, Editors, "Electrochemistry and Materials Science of Cathodic Hydrogen Absorption and Adsorption", **PV 94-21**, *The Electrochemical Society*, Pennington, NJ (1995).
5. D.M. Kolb, "Prog. Surf. Sci." **51**, 109 (1996).
6. G. Jerkiewicz, A. Zolfaghari, *J. Electrochem. Soc.* **143**, 1240 (1996).
7. A. Zolfaghari, F. Villiard, M. Chayer, G. Jerkiewicz, *J. Alloys Comp.* **253-254**, 481 (1997).
8. G. Jerkiewicz, *Prog. Surf. Sci.* **57**, 137 (1998).
9. M. W. Breiter, G. Staikov, W. J. Lorenz, "Electrochemistry and Materials Science of Cathodic Hydrogen Absorption and Adsorption", B. E. Conway, G. Jerkiewicz, Editors, **PV 94-21**, 152, *The Electrochemical Society*, Pennington, NJ (1995).
10. D. A. Harrington, B. E. Conway, *Electrochim. Acta.* **32**, 1703 (1987).
11. J. Barber, S. Morin, B. E. Conway, *J. Electroanal. Chem.* **446**, 125 (1998).
12. G. Jerkiewicz, A. Zolfaghari, *J. Phys. Chem.* **100**, 8454 (1996).
13. A. Zolfaghari, M. Chayer, G. Jerkiewicz, *J. Electrochem. Soc.* **144**, 3034 (1997).
14. S. Morin, H. Dumont, B. E. Conway, *J. Electroanal. Chem.* **412**, 39 (1996).
15. A. Zolfaghari, G. Jerkiewicz, *J. Electroanal. Chem.* **467**, 177 (1999).
16. G. Jerkiewicz, A. Zolfaghari, "Electrochemistry and Materials Science of Cathodic Hydrogen Absorption and Adsorption", B. E. Conway, G. Jerkiewicz, Editors, **PV 94-21**, 31, *The Electrochemical Society*, Pennington, NJ (1995).
17. B. E. Conway, "Interfacial Electrochemistry", A. Wieckowski, Editor, 131, Marcel Dekker, New York (1999).
18. E. Gileadi, "Electrosorption", E. Gileadi, Editor, 1, Plenum, New York (1967).
19. J. H. Chun, K. H. Ra, *J. Electrochem. Soc.* **145**, 3794 (1998).
20. J. H. Chun, K. H. Ra, "Hydrogen at Surfaces and Interfaces", G. Jerkiewicz, J. M. Feliu, B. N. Popov, Editors, **PV 2000-16**, 159, *The Electrochemical Society*, Pennington, NJ (2000).
21. J. H. Chun, S. K. Jeon, *J. Korean Electrochem. Soc.* **4**, 14 (2001).
22. J. H. Chun, K. H. Ra, N. Y. Kim, *Int. J. Hydrogen Energy*, **26**, 941

- (2001).
23. E. Gileadi, E. Kirowa-Eisner, J. Penciner, "Interfacial Electrochemistry", 72, Addison-Wesley Pub. Co., Reading, MA (1975).
  24. B. E. Conway, G. Jerkiewicz, *Electrochim. Acta.* **45**, 4075 (2000).
  25. B. E. Conway, G. Jerkiewicz, "Hydrogen at Surfaces and Interfaces", G. Jerkiewicz, J. M. Feliu, B. N. Popov, Editors, **PV 2000-16**, 1, The Electrochemical Society, Pennington, NJ (2000).
  26. E. Gileadi, E. Kirowa-Eisner, J. Penciner, "Interfacial Electrochemistry", 89, Addison-Wesley Pub. Co., Reading, MA (1975).
  27. D. D. MacDonald, "Transient Techniques in Electrochemistry", 298, Plenum Press, New York (1977).
  28. J. R. Scully, D. C. Silverman, M. W. Kendig, Editors, "Electrochemical Impedance: Analysis and Interpretation", ASTM, Philadelphia, PA, (1993).
  29. E. Gileadi, "Electrode Kinetics", 293, VCH, New York (1993).
  30. S. Sarangapani, B. V. Tilak, C. P. Chen, *J. Electrochem. Soc.* **143**, 3791 (1996).
  31. S. S. Buttarello, G. Tremiliosi-Filho, E. R. Gonzalez, "Electrochemistry and Materials Science of Cathodic Hydrogen Absorption and Adsorption", B. E. Conway, G. Jerkiewicz, Editors, **PV 94-21**, 299, The Electrochemical Society, Pennington, NJ (1995).
  32. R. D. Armstrong, M. Henderson, *J. Electroanal. Chem.* **39**, 81 (1972).
  33. J. H. Chun, K. H. Mun, C. D. Cho, *J. Korean Electrochem. Soc.* **3**, 25 (2000).
  34. A. J. Apple, "Comprehensive Treatise of Electrochemistry", B. E. Conway, J. O. M. Bockris, E. Yeager, S. U. M. Khan, R. E. White, Editors, Vol. 7, 218, Plenum Press, New York (1983).
  35. E. Gileadi, "Electrode Kinetics", 261, VCH, New York (1993).